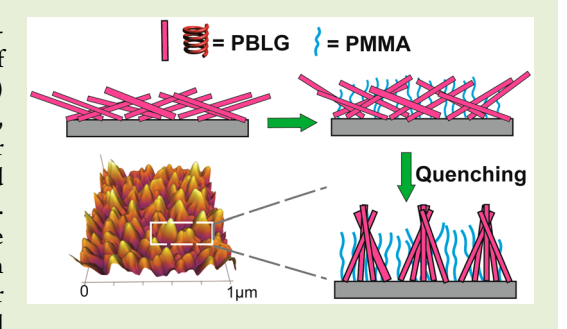
Synthesis, Processing, and Characterization of Helical Polypeptide Rod-Coil Mixed Brushes

Hai Tran,[†] Yiren Zhang,[‡] and Christopher K. Ober*,[‡]

[†]Robert F. Smith School of Chemical and Biomolecular Engineering and [‡]Department of Materials Science and Engineering, Cornell University, Ithaca, New York 14853, United States

Supporting Information

ABSTRACT: Mixed polymer brushes of rod-type polypeptide and coiltype vinyl polymer brushes were synthesized via two sequential steps of vapor deposition surface-initiated ring-opening polymerization (SI-ROP) and surface-initiated atom transfer radical polymerization (SI-ATRP), respectively. The effect on polypeptide brushes by coil-type brushes of their surface morphology, film thickness, and orientation were investigated before and after solvent quenching processes using chloroform and acetone. Before solvent quenching, the as-grown coil-type brushes forced the polypeptide brushes to stand up from the surface, resulting in higher film thickness, but the polypeptide brushes remained randomly oriented. After solvent quenching, polypeptide brushes tended to aggregate into conical



bundles with an orientation perpendicular to the substrate, but coil-type brushes restricted the free arrangement of the polypeptide brushes and lessen their upward movement. Changes in film thickness, rod orientation, morphology, and wettability were observed with increased molecular weight of the coil-type polymer in the mixed brushes.

oil-type polymer brushes are flexible but only form a planar surface morphology, which restricts access by big molecules to surface functional groups on the flat, crowded surface in a variety of possible applications. In contrast, polypeptide rod brushes mixed with coil polymer brushes, by combining high persistence length rod segments in brush layers of coil chains, offer numerous possibilities in applications dealing with surface structure and control. The mismatch in rigidity combined with controlled chain length gives rod brushes the potential to project a chain end with its specific chemical functionality from the coil-phase surface. Thus, specific functional groups can be distributed at an elevated height above a surface and at a reduced spacing to give the opportunity to explore conjugation with a target molecule such as an antibody or DNA. Moreover, coil brushes (in combination with rod brushes) may possess properties to prevent nonspecific adsorption making such combined materials of interest for molecular recognition and studies of cell-surface interaction. However, rod brushes will not stand up from the surface without intervention. In this study, we demonstrated the use of both solvent treatment and coil brushes to control the orientation of rod brushes as well as the size and number of rod assemblies. Through this control, brush surface morphology and surface properties can be tuned.

In this study, α -helical polypeptide brushes were used as models for rod polymers in general. Polypeptides are biocompatible and biodegrable, thus making them suited for several biological applications 1,2 The poly(γ-benzyl-L-glutamate) (PBLG) rod was used in this study as it has an α -helical conformation which is the most thermodynamically stable conformation.³ In contrast, poly(methyl methacrylate)

(PMMA) used as the second brush is one of the most common vinyl coil forming polymers. The PBLG polypeptide and PMMA brushes were grown from mixed initiators using the grafting-from approach via SI-ROP of α -amino acid Ncarboxyanhydrides (NCAs) and SI-ATRP, respectively. The grafting-from approaches were used to ensure a homogeneous and high grafting density film of polymer brushes. 4-7 In SI-ROP, the immobilized amine initiators on the surface will initiate a polymerization by reacting with NCA monomers to form the amide bond and release carbon dioxide while creating a new amine group at the end of the growing chain.⁵ In this study, the PBLG brushes were prepared via a vapor-phase approach mainly to produce homogeneous, well controlled thick films of polypeptides.^{3,8–12} SI-ATRP was used to grow coil-type brushes because this versatile technique can produce well-controlled polymer brushes for a wide range of monomers under mild conditions.4,13

Our preliminary test indicated that the two polymerization reactions are orthogonal, so no PBLG brushes can be grown from ATRP initiator and vice versa. Moreover, the ATRP initiators remained reactive after exposure to SI-ROP conditions as PMMA brushes were successfully grown with similar thickness under same conditions compared to a control sample. In addition, previous studies of polypeptide rod-coil block copolymers and bottlebrush polymers indicated the high stability of polypeptide under ATRP polymerization con-

Received: August 10, 2018 Accepted: September 10, 2018 Published: September 17, 2018

1186

ACS Macro Letters

Letter

Scheme 1. Synthesis Procedure to Make PBLG Rod/PMMA Coil Mixed Brushes

ditions, 14,15 which was also confirmed for PBLG brushes in our preliminary results. Therefore, the synthesis of mixed brushes was possible, but SI-ROP was carried out before SI-ATRP to avoid a diffusion problem of monomer molecules in the vapor phase toward reaction sites in the presence of PMMA brushes.

The deposition process to form mixed initiators was also considered. 3-Aminopropyldimethylethoxysilane (APDMES) was used as initiator for SI-ROP to ensure a monolayer of initiator. A two-step deposition was used. ATRP initiator was first deposited on surface to form a uniform, homogeneous layer of the initiator. Subsequently, APDMES was reacted with remaining active silanols on surface (Scheme 1). As APDMES and ATRP initiators contain nitrogen and bromine, respectively, in this study the ratio of N/Br, which was determined as 1.65 using XPS should be close to the composition of the mixed initiators on the surface.

Using the approaches mentioned above for the initiator depositions and polymerizations, mixed PBLG/PMMA brushes were successfully synthesized. The presence of both types of brushes was confirmed with FT-IR. For PBLG brushes, α -helical conformation has characteristic peaks of amide I (1654 cm⁻¹, backbone carbonyl stretching), amide II (1550 cm⁻¹,C-N stretching), amide A (3290 cm⁻¹, backbone N-H stretching), and the ester side chain (1734 cm⁻¹). 8,16,17 The FT-IR spectra of mixed brushes contained those peaks, indicating the presence of PBLG brushes in the α -helical conformation. In addition, the significant increase in intensity of the ester side chain (1734 cm⁻¹) and the presence of peak of CH₃ (2997 cm⁻¹, C-H stretching) suggested the addition of PMMA brushes (Figures 1 and S1).

In order to understand the interaction between PBLG and PMMA brushes, a systematic study was carried out based on the assumption that PMMA growth kinetics are not affected significantly by the presence of rod brushes. Various PMMA brush thicknesses were achieved via varying ATRP reaction time for substrates with the same rod brush thickness, which was defined as the measured thickness before the growth of PMMA brushes. In this work, a sample with an initial PBLG thickness of 62 nm was cut into four smaller samples (I–IV) from that surface PMMA brushes with different thicknesses ranging from 0, 31, and 61 to 107 nm for samples I–IV respectively were grown as determined from control samples of PMMA brushes (Figure 2). Interestingly, the final thickness of mixed brush samples was significantly higher than either PBLG

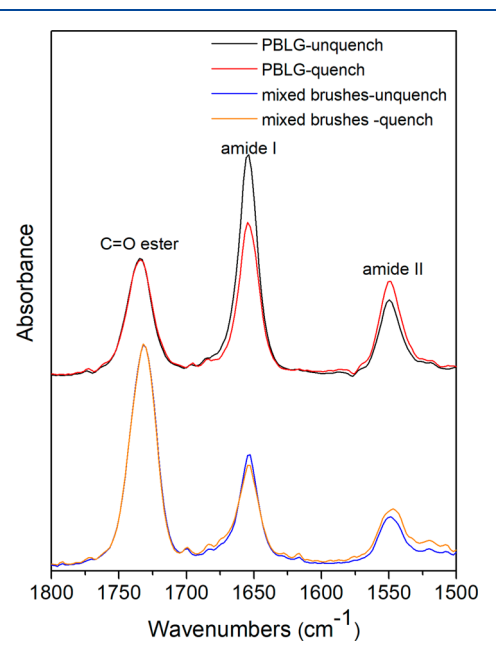


Figure 1. FT-IR transmission spectra of PBLG homopolymer brushes (top) and mixed brushes (bottom) before and after solvent quenching.

or PMMA control thickness. For example, the final thickness of sample IV were 142 nm, larger than that of PBLG (62 nm) and PMMA control (107 nm), respectively. To gain more insight of final thicknesses of mixed brushes, surface compositions of mixed brushes were studied using XPS to know if the PMMA or PBLG layer was at the topmost surface (Figure S2). XPS showed that a significant percentage of nitrogen retained in the topmost layer of all the samples, indicating that PBLG brushes remained as major component (Table 1). Considering the significant change in mixed brush thickness, we hypothesized that the presence of PMMA brushes changed the orientation of PBLG brushes to more upright orientation, thus increasing the thickness. Initially, the PBLG brushes tend to orient parallel to the surface to minimize surface energy, 16 but PMMA brushes occupied the space and forced PBLG brushes to be more perpendicular from the surface. Thus, the final thickness was the new thickness of PBLG brushes at higher tilt angle.

This hypothesis can also be supported by FT-IR measurements in transmission mode, since the intensity of the amide

ACS Macro Letters Letter

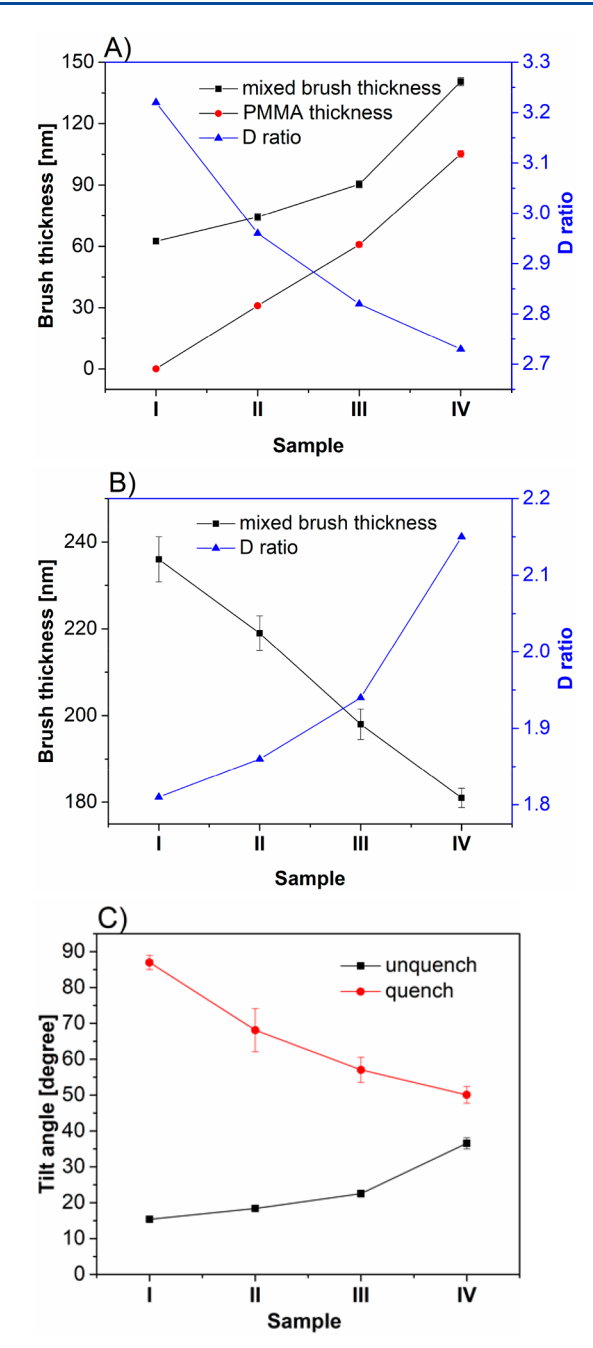


Figure 2. Thickness of PMMA and mixed brushes, and the D ratio for (A) before solvent quenching and (B) after solvent quenching; (C) tilt angle between the PBLG helices and the substrate before and after solvent quenching. The D value is defined as the ratio of amide I to amide II peak intensity. The samples have the same molecular weight of PBLG but increasing thickness of PMMA from sample I to IV. The angle of quenched PBLG brushes (sample I) was assumed to be 87° as in ref 18.

bonds changes with polypeptide orientation. The transition dipole moments with respect to an α -helix backbone are 39° and 75° for amide I and amide II, respectively. Thus, under the transmission mode, when the IR-beam went through the samples and interacted with PBLG brushes, only the active electric field components of the transition dipole moments of the amide bonds parallel to the substrate were measured. Then, the dichroic ratio D of amide I over amide II adsorption can give a qualitative assessment of the average orientation of

Table 1. Surface Composition of Mixed Brush Samples Measured with XPS before Solvent Quenching^a

| | ATRP reaction time (h) | C% | N% | Ο% |
|------------|------------------------|-------|------|-------|
| sample I | 0 | 72.24 | 6.64 | 21.12 |
| sample II | 4 | 71.94 | 4.95 | 23.11 |
| sample III | 8 | 69.80 | 5.26 | 24.94 |
| sample IV | 20 | 69.58 | 4.69 | 25.73 |

^aThe samples have the same molecular weight of PBLG but increased thickness of PMMA from sample I to sample IV by varying the ATRP reaction time.

 α -helical rod. $^{17-19}$ The decrease in D value is related to higher average tilt angle of the α -helical rods with respect to the substrate. The trend of decreasing D value from sample I to IV implied an increase in average tilt angle which was consistent with the increase in film thickness mentioned previously (Figures 1 and 2A). AFM images showed homogeneous and quite smooth surfaces for all samples (Figure S3) and indicated disordered orientations of PBLG brushes. Lastly, the water contact angle of the samples was also measured. No obvious change of water contact angle was observed from samples I–IV (Figure 3).

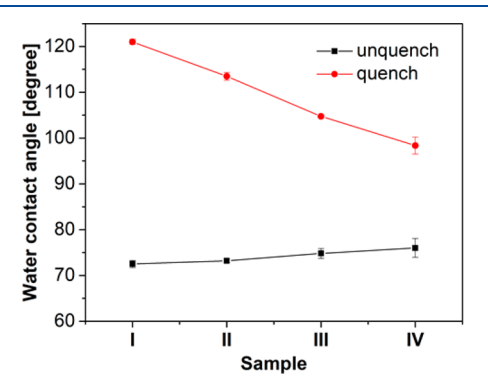


Figure 3. Water contact angle of mixed brush samples before and after solvent quenching.

Subsequently, a processing step called "solvent quenching" was applied to enhance PBLG orientational order and aggregation.¹⁸ Mixed brush samples were first immersed in chloroform, a good solvent for PBLG to cause the chains to stand up before immediately transferring the samples into acetone, a bad solvent for PBLG so that the PBLG brushes would aggregate to minimize contact with acetone, thereby freezing any vertical orientation of PBLG brushes (Figure 4A). 18,20 After solvent quenching, a dramatic change in thickness was observed for all the samples (Figure 2B). However, the change in thickness was less significant for an increase in thickness of PMMA brushes, indicating a smaller change in the angle between the α -helix rod and the substrate. Our hypothesis was that the presence of PMMA brushes acted as a constraint on the rearrangement of PBLG brushes during solvent quenching. For sample I, PBLG brushes alone freely moved from parallel to perpendicular orientation while the entanglement of PMMA brushes made it harder for PBLG rods to move upright as seen in the samples II-IV. The dichroic ratio D again supported this hypothesis. The increase in D value from sample I-IV after solvent quenching indicated that the orientation of PBLG rods over the substrate was less perpendicular.

ACS Macro Letters

Letter

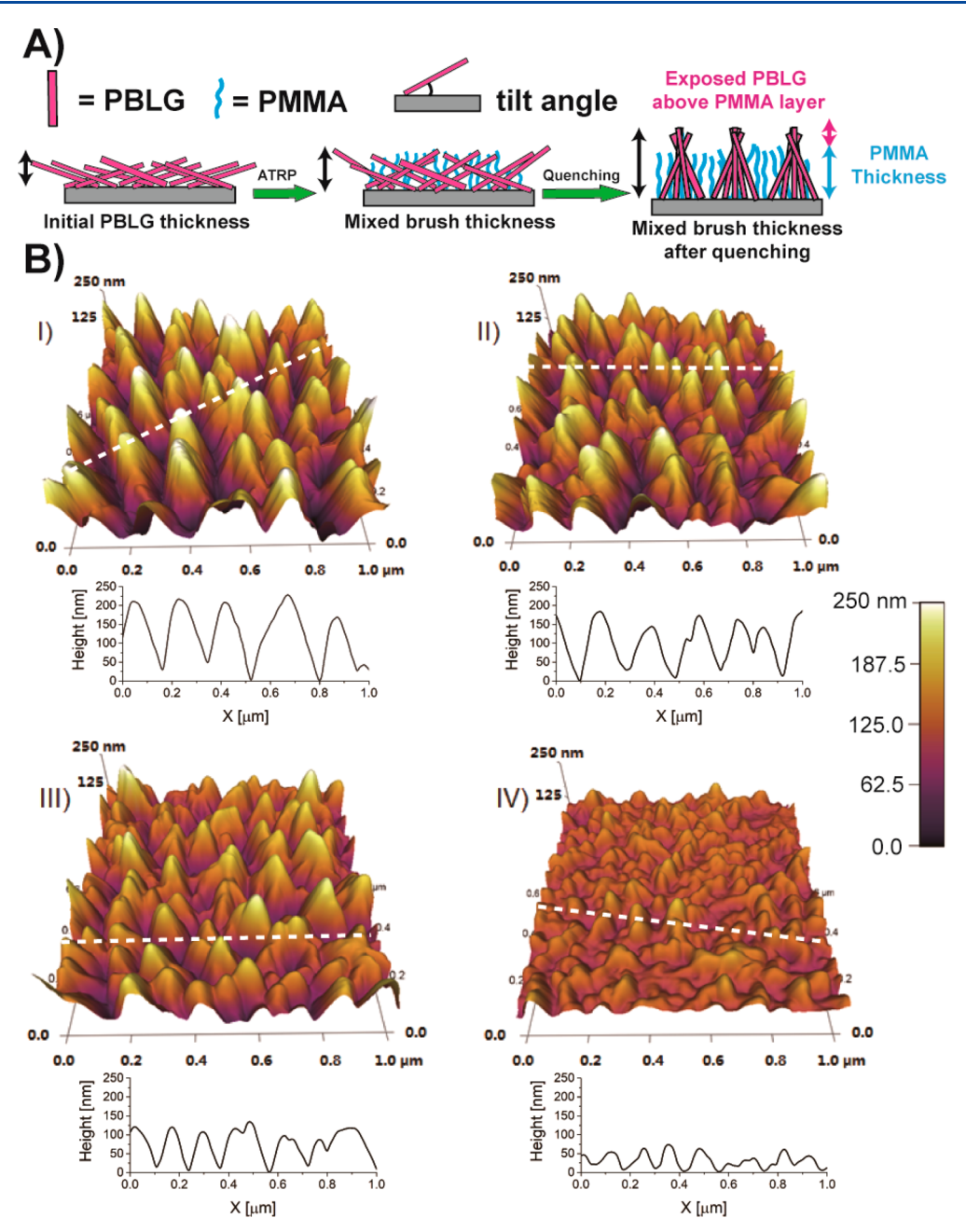


Figure 4. (A) Schematic figure of rod—coil mixed brushes; (B) The height images and cross-sectional profiles of mixed polymer brushes after solvent quenching. The white dashed lines in the height images indicate the cross-sectional height measurement of the accompanying height profiles. All samples have the same molecular weight of polypeptide brushes but increased thickness of PMMA from sample I to sample IV. The scan size is $1 \ \mu m \times 1 \ \mu m$.

Previous studies reported an almost perpendicular orientation of PBLG brushes after solvent quenching. 18,20 Thus, we assume that the final thickness of PBLG homopolymer brushes (sample I, 235 nm) after solvent quenching should be nearly equal to the length of the PBLG brushes. As each monomer unit contributes 1.5 Å along the helical axis of the chain to the final length of PBLG brushes, the degree of polymerization was about 1500. 17 Using the PBLG density of 1.32 g/cm³, 11 the grafting density of PBLG helices was estimated as 0.143 chain/nm, while the grafting density of PMMA brushes calculated from molecular weight (MW) of free polymer was 0.56 chain/nm. 222,23 The tilt angle of PBLG rods in mixed brushes was ranged from 16° to 38° before quenching and from 87° to 51° after quenching (Figure 2C).

AFM images also gave more information about mixed brush structure after solvent quenching. In particular, conical aggregates were observed for all the samples, though the height and sizes of aggregates varied from the samples I–IV (Figure 4B). The average height of the aggregates and the spacing between neighboring aggregates grew smaller while the total number of aggregates per μm^2 increased from 42 to 98 aggregates going from sample I to sample IV (Table S1). The presence of PMMA brushes disrupted the aggregation process, so only nearby PBLG rods could interact with each other to form aggregate bundles. The higher number of aggregates in mixed brushes may allow more chain-end functional groups of the PBLG rods to project from the surface. Moreover, the aggregates looked smaller and shorter in the mixed brushes

ACS Macro Letters

Letter

because their lower parts were buried by the PMMA brush layer and became invisible to AFM (Figure 4A). Thus, with an increase in thickness of the PMMA layer from samples I to IV, the exposed part of the aggregates was smaller.

The water contact angle after quenching changed significantly. Sample I changed from 72.5° to 121°. This drastic change may be due to the formation of nanostructured rod aggregates. A similar effect was observed for lotus leaves when papillae structures of a leave can trap air when contacting water drops and make the leaf superhydrophobic.²⁴ However, the addition of PMMA lowered the hydrophobicity as the angle of sample IV was 98°. At higher thickness of PMMA brushes, a higher volume of PBLG brushes was buried under a PMMA layer, thereby reducing the surface roughness (Table S1).

In conclusion, we have reported the study of mixed polymer brushes consisting of α -helical polypeptide rod and vinyl-type polymer coil. With constant starting rod PBLG thickness, the final thickness of mixed brushes prior to solvent quenching increase monotonically with the increase in MW of coil type PMMA brushes due to a change in the orientation of PBLG rods. After solvent quenching, a significant increase in thickness was observed due to the formation of the conical aggregates of PBLG rods. However, monotonical decrease in the final thickness was seen because the entanglement of PMMA brushes restricted the movement of PBLG rods. As a result, less perpendicular rods were observed with an increase of PMMA brush thickness. Consequently, surface morphology and hydrophobicity also changed dramatically. Our studies showed that rod-coil mixed brushes behave differently from coil-coil mixed brushes, which have a subtle difference in height between two coil phases.^{22,25} This rod-coil system can lead to unique types of phase separation which can bring more chain-end functional groups of rod brushes to air interface. The versatility of ATRP polymerization and the high stability of polypeptides under ATRP conditions demonstrated in our study showed the potential of stimuli-responsive coil-type brushes or block copolymer brushes in a rod-coil system.

ASSOCIATED CONTENT

S Supporting Information

The Supporting Information is available free of charge on the ACS Publications website at DOI: 10.1021/acsmacrolett.8b00606.

Synthesis, characterization methods, additional AFM, FT-IR and XPS data, and calculation of polymer grafting density (PDF).

AUTHOR INFORMATION

Corresponding Author

*E-mail cko3@cornell.edu.

ORCID 6

Christopher K. Ober: 0000-0002-3805-3314

Funding

This work is supported by the National Science Foundation (DMR-1506542 and CHE-1709660).

Notes

The authors declare no competing financial interest.

ACKNOWLEDGMENTS

The authors would like to acknowledge fruitful discussions with Prof. Su-mi Hur. This work made use of the Cornell

Center for Materials Research Shared Facilities which are supported through the NSF MRSEC Program (DMR-1719875) and Cornell NanoScale Facility, an NNCI member supported by NSF Grant NNCI-1542081.

REFERENCES

- (1) Kar, M.; Pauline, M.; Sharma, K.; Kumaraswamy, G.; Sen Gupta, S. Synthesis of Poly- 1 -Glutamic Acid Grafted Silica Nanoparticles and Their Assembly into Macroporous Structures. *Langmuir* **2011**, 27 (19), 12124–12133.
- (2) Ma, Y.; Shen, Y.; Li, Z. Different Cell Behaviors Induced by Stereochemistry on Polypeptide Brush Grafted Surfaces. *Mater. Chem. Front* **2017**, *1* (5), 846–851.
- (3) Lee, N. H.; Frank, C. W. Surface-Initiated Vapor Polymerization of Various α -Amino Acids. *Langmuir* **2003**, *19* (4), 1295–1303.
- (4) Barbey, R.; Lavanant, L.; Paripovic, D.; Schüwer, N.; Sugnaux, C.; Tugulu, S.; Klok, H.-A. Polymer Brushes via Surface-Initiated Controlled Radical Polymerization: Synthesis, Characterization, Properties, and Applications. *Chem. Rev.* **2009**, *109* (11), 5437–5527.
- (5) Wibowo, S. H.; Sulistio, A.; Wong, E. H. H.; Blencowe, A.; Qiao, G. G. Polypeptide Films via N-Carboxyanhydride Ring-Opening Polymerization (NCA-ROP): Past, Present and Future. *Chem. Commun.* **2014**, *50* (39), 4971.
- (6) Shen, Y.; Li, Z.; Klok, H.-A. Polypeptide Brushes Grown via Surface-Initiated Ring-Opening Polymerization of α -Amino Acid N-Carboxyanhydrides. *Chin. J. Polym. Sci.* **2015**, 33 (7), 931–946.
- (7) Chen, W.-L.; Cordero, R.; Tran, H.; Ober, C. K. *50th Anniversary Perspective*: Polymer Brushes: Novel Surfaces for Future Materials. *Macromolecules* **2017**, *50* (11), 4089–4113.
- (8) Chang, Y.-C.; Frank, C. W. Vapor Deposition- Polymerization of α -Amino Acid N-Carboxy Anhydride on the Silicon (100) Native Oxide Surface. *Langmuir* **1998**, *14* (2), 326–334.
- (9) Zheng, W.; Frank, C. W. Surface-Initiated Vapor Deposition Polymerization of Poly(γ -Benzyl-l-Glutamate): Optimization and Mechanistic Studies. *Langmuir* **2010**, 26 (6), 3929–3941.
- (10) Shen, Y.; Desseaux, S.; Aden, B.; Lokitz, B. S.; Kilbey, S. M.; Li, Z.; Klok, H.-A. Shape-Persistent, Thermoresponsive Polypeptide Brushes Prepared by Vapor Deposition Surface-Initiated Ring-Opening Polymerization of α -Amino Acid N -Carboxyanhydrides. *Macromolecules* **2015**, 48 (8), 2399–2406.
- (11) Wang, Y.; Chang, Y.-C. Grafting of Homo- and Block Co-Polypeptides on Solid Substrates by an Improved Surface-Initiated Vapor Deposition Polymerization. *Langmuir* **2002**, *18* (25), 9859–9866.
- (12) Yang, C.-T.; Wang, Y.; Chang, Y.-C. Effect of Solvents and Temperature on the Conformation of Poly(β -Benzyl- l -Aspartate) Brushes. *Biomacromolecules* **2010**, *11* (5), 1308–1313.
- (13) Khabibullin, A.; Mastan, E.; Matyjaszewski, K.; Zhu, S. Surface-Initiated Atom Transfer Radical Polymerization. In *Controlled Radical Polymerization at and from Solid Surfaces*; Vana, P., Ed.; Springer International Publishing: Cham, 2015; Vol. 270, pp 29–76.
- (14) Huang, C.-J.; Chang, F.-C. Polypeptide Diblock Copolymers: Syntheses and Properties of Poly(N-Isopropylacrylamide)-b-Polylysine. *Macromolecules* **2008**, *41* (19), 7041–7052.
- (15) Ding, J.; Xiao, C.; Tang, Z.; Zhuang, X.; Chen, X. Highly Efficient "Grafting From" an α -Helical Polypeptide Backbone by Atom Transfer Radical Polymerization. *Macromol. Biosci.* **2011**, *11* (2), 192–198.
- (16) Wieringa, R. H.; Siesling, E. A.; Geurts, P. F. M.; Werkman, P. J.; Vorenkamp, E. J.; Erb, V.; Stamm, M.; Schouten, A. J. Surface Grafting of Poly (L-Glutamates). 1. Synthesis and Characterization. *Langmuir* **2001**, *17* (21), 6477–6484.
- (17) Wieringa, R. H.; Siesling, E. A.; Werkman, P. J.; Angerman, H. J.; Vorenkamp, E. J.; Schouten, A. J. Surface Grafting of Poly(l-Glutamates). 2. Helix Orientation. *Langmuir* **2001**, *17* (21), 6485–6490.

ACS Macro Letters Letter

(18) Wang, Y.; Chang, Y. C. Preparation of Unidirectional End-Grafted α -Helical Polypeptides by Solvent Quenching. *J. Am. Chem. Soc.* **2003**, 125 (21), 6376–6377.

- (19) Vlasova, E.; Volchek, B.; Tarasenko, I.; Vlasov, G. Spectroscopic Investigation of Polypeptide Plane Brushes. *Macromol. Symp.* **2011**, 305 (1), 116–121.
- (20) Wu, J.-C.; Chen, C.-C.; Chen, K.-H.; Chang, Y.-C. Controlled Growth of Aligned α-Helical-Polypeptide Brushes for Tunable Electrical Conductivity. *Appl. Phys. Lett.* **2011**, *98* (13), 133304.
- (21) Machida, S.; Urano, T. I.; Sano, K.; Kawata, Y.; Sunohara, K.; Sasaki, H.; Yoshiki, M.; Mori, Y. A Chiral Director Field in the Nematic Liquid Crystal Phase Induced by a Poly(.Gamma.-Benzyl Glutamate) Chemical Reaction Alignment Film. *Langmuir* 1995, 11 (12), 4838–4843.
- (22) Zhao, B. Synthesis of Binary Mixed Homopolymer Brushes by Combining Atom Transfer Radical Polymerization and Nitroxide-Mediated Radical Polymerization. *Polymer* **2003**, *44* (15), 4079–4083.
- (23) Ionov, L.; Minko, S. Mixed Polymer Brushes with Locking Switching. ACS Appl. Mater. Interfaces 2012, 4 (1), 483–489.
- (24) Sun, T.; Feng, L.; Gao, X.; Jiang, L. Bioinspired Surfaces with Special Wettability. *Acc. Chem. Res.* **2005**, 38 (8), 644–652.
- (25) Price, A. D.; Hur, S.-M.; Fredrickson, G. H.; Frischknecht, A. L.; Huber, D. L. Exploring Lateral Microphase Separation in Mixed Polymer Brushes by Experiment and Self-Consistent Field Theory Simulations. *Macromolecules* **2012**, *45* (1), 510–524.